Numerical kludge waveforms for scoping out LISA data analysis

Jonathan Gair, IoA, Cambridge

Kostas Glampedakis (Soton), Scott Hughes (MIT)

Stas Babak (AEI), Hua Fang (Caltech)

Capra 8, Abingdon, 13th July 2005

Talk outline

- The need for waveform approximations.
- "Numerical kludge" approach to waveform computation.
  - ⋆ Description of method.
  - ⋆ Generation of phase space trajectories.
  - ⋆ Computation of corresponding gravitational waves.
- Tests of the numerical kludge results.
- Present and future applications of kludge waveforms.

The need for approximate waveforms

- EMRIs are an exciting source for LISA – provide an unprecedented probe of black hole spacetimes, waveforms in principle are well understood.

The need for approximate waveforms

- EMRIs are an exciting source for LISA – provide an unprecedented probe of black hole spacetimes, waveforms in principle are well understood.

- EMRI parameter space is very large (17 dimensional parameter space of signals). Inspiral signals have long duration (several years). Fully coherent matched filtering is therefore impossible with realistic computational resources.

The need for approximate waveforms

- EMRIs are an exciting source for LISA – provide an unprecedented probe of black hole spacetimes, waveforms in principle are well understood.

- EMRI parameter space is very large (17 dimensional parameter space of signals). Inspiral signals have long duration (several years). Fully coherent matched filtering is therefore impossible with realistic computational resources.

- Must employ alternative algorithms for LISA data analysis (see talk tomorrow). Need waveform templates to explore and optimize these algorithms.

The need for approximate waveforms

- EMRIs are an exciting source for LISA – provide an unprecedented probe of black hole spacetimes, waveforms in principle are well understood.
- EMRI parameter space is very large (17 dimensional parameter space of signals). Inspiral signals have long duration (several years). Fully coherent matched filtering is therefore impossible with realistic computational resources.
- Must employ alternative algorithms for LISA data analysis (see talk tomorrow). Need waveform templates to explore and optimize these algorithms.
- Perturbative waveforms have been computed for certain cases (and generic adiabatic templates should soon be available - see Drasco talk). However, these codes are slow.

The need for approximate waveforms

- Computation of template space metrics requires evaluation of waveform derivatives, and metric eigenvalues vary by many orders of magnitude – must compute many nearby waveforms and iterate at each point in parameter space.

The need for approximate waveforms

- Computation of template space metrics requires evaluation of waveform derivatives, and metric eigenvalues vary by many orders of magnitude – must compute many nearby waveforms and iterate at each point in parameter space.

- Need techniques to compute realistic waveforms quickly and cheaply – develop "kludge" approaches that capture the main features of EMR inspirals.

The need for approximate waveforms

- Computation of template space metrics requires evaluation of waveform derivatives, and metric eigenvalues vary by many orders of magnitude – must compute many nearby waveforms and iterate at each point in parameter space.

- Need techniques to compute realistic waveforms quickly and cheaply – develop "kludge" approaches that capture the main features of EMR inspirals.

- "Kludge" –

  ⋆ 'A system, especially a computer system, that is constructed of poorly matched elements or of elements originally intended for other applications' (American Heritage Dictionary).

The need for approximate waveforms

- Computation of template space metrics requires evaluation of waveform derivatives, and metric eigenvalues vary by many orders of magnitude – must compute many nearby waveforms and iterate at each point in parameter space.

- Need techniques to compute realistic waveforms quickly and cheaply – develop "kludge" approaches that capture the main features of EMR inspirals.

- "Kludge" –
  - ⋆ 'A system, especially a computer system, that is constructed of poorly matched elements or of elements originally intended for other applications' (American Heritage Dictionary).
  - ⋆ 'A clumsy or inelegant solution to a problem' (American Heritage Dictionary).

The need for approximate waveforms

- Computation of template space metrics requires evaluation of waveform derivatives, and metric eigenvalues vary by many orders of magnitude – must compute many nearby waveforms and iterate at each point in parameter space.

- Need techniques to compute realistic waveforms quickly and cheaply – develop "kludge" approaches that capture the main features of EMR inspirals.

- "Kludge" –
  - ⋆ 'A system, especially a computer system, that is constructed of poorly matched elements or of elements originally intended for other applications' (American Heritage Dictionary).
  - ⋆ 'A clumsy or inelegant solution to a problem' (American Heritage Dictionary).
  - ⋆ 'Something hastily or badly put together' (AskOxford.com).

"Analytic" kludge

Barack and Cutler (2004)

- Use Keplerian (Peters and Mathews) waveforms as a basis.

"Analytic" kludge

Barack and Cutler (2004)

- Use Keplerian (Peters and Mathews) waveforms as a basis.
- Add relativistic effects using post-Newtonian results
  - ⋆ Perihelion precession, precession of orbital plane.
  - ⋆ Evolution of orbital parameters (frequency, eccentricity) over the inspiral.

"Analytic" kludge

Barack and Cutler (2004)

- Use Keplerian (Peters and Mathews) waveforms as a basis.
- Add relativistic effects using post-Newtonian results
  - ⋆ Perihelion precession, precession of orbital plane.
  - ⋆ Evolution of orbital parameters (frequency, eccentricity) over the inspiral.
- Include low-frequency approximation to the LISA detector response.

"Analytic" kludge

Barack and Cutler (2004)

- Use Keplerian (Peters and Mathews) waveforms as a basis.
- Add relativistic effects using post-Newtonian results
  - ⋆ Perihelion precession, precession of orbital plane.
  - ⋆ Evolution of orbital parameters (frequency, eccentricity) over the inspiral.
- Include low-frequency approximation to the LISA detector response.
- Analytic kludge waveforms can be computed very quickly, but are hard to match onto perturbative computations.

"Numerical" kludge

- Compute a phase space trajectory by integrating a prescription for $\dot{E}$, $\dot{L}_z$ and $\dot{Q}$ as functions of E, L_z and Q (adiabatic approximation).

"Numerical" kludge

- Compute a phase space trajectory by integrating a prescription for $\dot{E}$, $\dot{L}_z$ and $\dot{Q}$ as functions of E, L_z and Q (adiabatic approximation).

- Integrate the Kerr geodesic equations numerically for resultant $E(t)$, $L_t(t)$ and $Q(t)$ to give $r(t)$, $\theta(t)$ and $\phi(t)$

$$
\begin{aligned}
\Sigma^2 \left(\frac{\mathrm{d}r}{\mathrm{d}\tau}\right)^2 &= \left[\left(r^2+a^2\right)E - aL_z\right]^2 - \Delta\left[r^2 + \left(L_z - aE\right)^2 + Q\right] \\
\Sigma^2 \left(\frac{\mathrm{d}\theta}{\mathrm{d}\tau}\right)^2 &= Q - \cot^2\theta\, L_z^2 - a^2\cos^2\theta\left(1-E^2\right) \\
\Sigma\left(\frac{\mathrm{d}\phi}{\mathrm{d}\tau}\right) &= \csc^2\theta L_z + aE\left(\frac{r^2+a^2}{\Delta} - 1\right) - \frac{a^2 L_z}{\Delta} \\
\Sigma\left(\frac{\mathrm{d}t}{\mathrm{d}\tau}\right) &= E\left[\frac{\left(r^2+a^2\right)^2}{\Delta} - a^2\sin^2\theta\right] + aL_z\left(1 - \frac{r^2+a^2}{\Delta}\right). \qquad (1)
\end{aligned}
$$

"Numerical" kludge

- Identify Boyer-Lindquist coordinates (r, θ, ϕ) with flat space spherical polar coordinates. Construct approximate gravitational waveform from resulting flat space quadrupole moment tensor ("particle on a string").

"Numerical" kludge

- Identify Boyer-Lindquist coordinates (r, θ, ϕ) with flat space spherical polar coordinates. Construct approximate gravitational waveform from resulting flat space quadrupole moment tensor ("particle on a string").

- Include detector modulations using low-frequency approximation to LISA response.

"Numerical" kludge

- Identify Boyer-Lindquist coordinates (r, θ, ϕ) with flat space spherical polar coordinates. Construct approximate gravitational waveform from resulting flat space quadrupole moment tensor ("particle on a string").

- Include detector modulations using low-frequency approximation to LISA response.

- Numerical kludge waveforms are more computationally intensive to generate than the analytic ones but

  ⋆ They may be easily identified with perturbative waveforms since they employ geodesic parameters.
  ⋆ The fundamental frequencies are instantaneously correct, since they are based on integration of the true Kerr geodesic equations.

Geodesic parameterization

- Instead of E, L_z and Q, we define a semi-latus rectum, p, an eccentricity, e, and an orbital inclination angle, ι.

Geodesic parameterization

- Instead of E, L_z and Q, we define a semi-latus rectum, p, an eccentricity, e, and an orbital inclination angle, ι.

- Find the extrema of the orbit, r_p and r_a, which are roots of the radial geodesic equation

$$R(r) = \left[\left(r^2 + a^2\right) E - aL_z\right]^2 - \Delta\left[r^2 + \left(L_z - aE\right)^2 + Q\right] \tag{2}$$

- Define p and e using the Keplerian definitions

$$r_p = \frac{p}{1+e}, \qquad r_a = \frac{p}{1-e} \qquad \Rightarrow \qquad e = \frac{r_a - r_p}{r_a + r_p}, \qquad p = \frac{2\, r_a\, r_p}{r_a + r_p} \tag{3}$$

- Define ι in terms of L_z and Q by $Q = L_z^2 \tan^2 \iota$.

Phase-space trajectories

- Basic idea (Glampedakis, Hughes & Kennefick 2002) – use post-Newtonian energy and angular momentum fluxes (from Ryan 1996)

$$
\begin{aligned}
\frac{\mathrm{d}E}{\mathrm{d}t} &= -\frac{32}{5}\frac{\mu^2}{M^2}\left(\frac{M}{p}\right)^5 (1-e^2)^{3/2}\left[f_1(e) - \frac{a}{M}\left(\frac{M}{p}\right)^{3/2}\cos\iota f_2(e)\right], \\
\frac{\mathrm{d}L_z}{\mathrm{d}t} &= -\frac{32}{5}\frac{\mu^2}{M}\left(\frac{M}{p}\right)^{7/2} (1-e^2)^{3/2}\left[\cos\iota f_3(e) + \frac{a}{M}\left(\frac{M}{p}\right)^{3/2}\left[f_4(e) - \cos^2\iota f_5(e)\right]\right] \\
f_1(e) &= 1 + \frac{73}{24}e^2 + \frac{37}{96}e^4, \qquad f_2(e) = \frac{73}{12} + \frac{823}{24}e^2 + \frac{949}{32}e^4 + \frac{491}{192}e^6, \qquad f_3(e) = 1 + \frac{7}{8}e^2, \\
f_4(e) &= \frac{61}{24} + \frac{63}{8}e^2 + \frac{95}{64}e^4, \qquad f_5(e) = \frac{61}{8} + \frac{91}{4}e^2 + \frac{461}{64}e^4, \qquad f_6(e) = \frac{97}{12} + \frac{37}{2}e^2 + \frac{211}{32}e^4
\end{aligned}
\tag{4}
$$

Phase-space trajectories

- Basic idea (Glampedakis, Hughes & Kennefick 2002) – use post-Newtonian energy and angular momentum fluxes (from Ryan 1996)

$$
\begin{aligned}
\frac{\mathrm{d}E}{\mathrm{d}t} &= -\frac{32}{5}\frac{\mu^2}{M^2}\left(\frac{M}{p}\right)^5 (1-e^2)^{3/2}\left[f_1(e) - \frac{a}{M}\left(\frac{M}{p}\right)^{3/2}\cos\iota f_2(e)\right], \\
\frac{\mathrm{d}L_z}{\mathrm{d}t} &= -\frac{32}{5}\frac{\mu^2}{M}\left(\frac{M}{p}\right)^{7/2} (1-e^2)^{3/2}\left[\cos\iota f_3(e) + \frac{a}{M}\left(\frac{M}{p}\right)^{3/2}\left[f_4(e) - \cos^2\iota f_5(e)\right]\right] \\
f_1(e) &= 1 + \frac{73}{24}e^2 + \frac{37}{96}e^4, \qquad f_2(e) = \frac{73}{12} + \frac{823}{24}e^2 + \frac{949}{32}e^4 + \frac{491}{192}e^6, \qquad f_3(e) = 1 + \frac{7}{8}e^2, \\
f_4(e) &= \frac{61}{24} + \frac{63}{8}e^2 + \frac{95}{64}e^4, \qquad f_5(e) = \frac{61}{8} + \frac{91}{4}e^2 + \frac{461}{64}e^4, \qquad f_6(e) = \frac{97}{12} + \frac{37}{2}e^2 + \frac{211}{32}e^4
\end{aligned}
\tag{4}
$$

- GHK took $i = 0$ since Ryan's i significantly overpredicted the change in inclination when compared to circular Teukolsky calculations by Hughes (2000).

Phase-space trajectories

- Basic idea (Glampedakis, Hughes & Kennefick 2002) – use post-Newtonian energy and angular momentum fluxes (from Ryan 1996)

$$
\begin{aligned}
\frac{\mathrm{d}E}{\mathrm{d}t} &= -\frac{32}{5}\frac{\mu^2}{M^2}\left(\frac{M}{p}\right)^5 (1-e^2)^{3/2}\left[f_1(e) - \frac{a}{M}\left(\frac{M}{p}\right)^{3/2}\cos\iota f_2(e)\right], \\
\frac{\mathrm{d}L_z}{\mathrm{d}t} &= -\frac{32}{5}\frac{\mu^2}{M}\left(\frac{M}{p}\right)^{7/2} (1-e^2)^{3/2}\left[\cos\iota f_3(e) + \frac{a}{M}\left(\frac{M}{p}\right)^{3/2}\left[f_4(e) - \cos^2\iota f_5(e)\right]\right] \\
f_1(e) &= 1 + \frac{73}{24}e^2 + \frac{37}{96}e^4, \qquad f_2(e) = \frac{73}{12} + \frac{823}{24}e^2 + \frac{949}{32}e^4 + \frac{491}{192}e^6, \qquad f_3(e) = 1 + \frac{7}{8}e^2, \\
f_4(e) &= \frac{61}{24} + \frac{63}{8}e^2 + \frac{95}{64}e^4, \qquad f_5(e) = \frac{61}{8} + \frac{91}{4}e^2 + \frac{461}{64}e^4, \qquad f_6(e) = \frac{97}{12} + \frac{37}{2}e^2 + \frac{211}{32}e^4
\end{aligned} \tag{4}
$$

- GHK took $i = 0$ since Ryan's i significantly overpredicted the change in inclination when compared to circular Teukolsky calculations by Hughes (2000).

- This approach exhibits some pathological behaviour. This arises because necessary cancellations do not occur when using accurate parameter specification for (p, e, ι) with PN fluxes. Must add corrections to enforce these cancellations.

Consistency corrections – near circular orbits

- Eccentricity evolution is given from the fluxes

$$\frac{\mathrm{d}e}{\mathrm{d}t} = \frac{\partial e}{\partial E}\frac{\mathrm{d}E}{\mathrm{d}t} + \frac{\partial e}{\partial L_z}\frac{\mathrm{d}L_z}{\mathrm{d}t} + \frac{\partial e}{\partial \iota}\frac{\mathrm{d}\iota}{\mathrm{d}t} \tag{5}$$

Consistency corrections – near circular orbits

- Eccentricity evolution is given from the fluxes

$$\frac{\mathrm{d}e}{\mathrm{d}t} = \frac{\partial e}{\partial E}\frac{\mathrm{d}E}{\mathrm{d}t} + \frac{\partial e}{\partial L_z}\frac{\mathrm{d}L_z}{\mathrm{d}t} + \frac{\partial e}{\partial \iota}\frac{\mathrm{d}\iota}{\mathrm{d}t} \tag{5}$$

- Definition of parameters ensures E, L_z, $\dot{E}$ and $\dot{L}_z$ are functions of p, e^2 and ι only $\Rightarrow \mathrm{d}e/\mathrm{d}t \propto 1/e$ unless cancellations occur.

Consistency corrections – near circular orbits

- Eccentricity evolution is given from the fluxes

$$\frac{\mathrm{d}e}{\mathrm{d}t} = \frac{\partial e}{\partial E}\frac{\mathrm{d}E}{\mathrm{d}t} + \frac{\partial e}{\partial L_z}\frac{\mathrm{d}L_z}{\mathrm{d}t} + \frac{\partial e}{\partial \iota}\frac{\mathrm{d}\iota}{\mathrm{d}t} \tag{5}$$

- Definition of parameters ensures E, L_z, $\dot{E}$ and $\dot{L}_z$ are functions of p, e^2 and ι only $\Rightarrow \mathrm{d}e/\mathrm{d}t \propto 1/e$ unless cancellations occur.

- These cancellations are precisely what is required to make $\mathrm{d}e/\mathrm{d}t = 0$ for circular orbits. This is the condition that circular orbits remain circular under radiation reaction, which has to hold for physical inspirals (Kennefick & Ori 1998).

Consistency corrections – near circular orbits

- Eccentricity evolution is given from the fluxes

$$\frac{\mathrm{d}e}{\mathrm{d}t} = \frac{\partial e}{\partial E}\frac{\mathrm{d}E}{\mathrm{d}t} + \frac{\partial e}{\partial L_z}\frac{\mathrm{d}L_z}{\mathrm{d}t} + \frac{\partial e}{\partial \iota}\frac{\mathrm{d}\iota}{\mathrm{d}t} \tag{5}$$

- Definition of parameters ensures E, L_z, $\dot{E}$ and $\dot{L}_z$ are functions of p, e^2 and ι only $\Rightarrow \mathrm{d}e/\mathrm{d}t \propto 1/e$ unless cancellations occur.

- These cancellations are precisely what is required to make $\mathrm{d}e/\mathrm{d}t = 0$ for circular orbits. This is the condition that circular orbits remain circular under radiation reaction, which has to hold for physical inspirals (Kennefick & Ori 1998).

- In GHK, the constraint holds only at the PN order of the fluxes – leads to unphysical features.

Near circular orbits – no correction

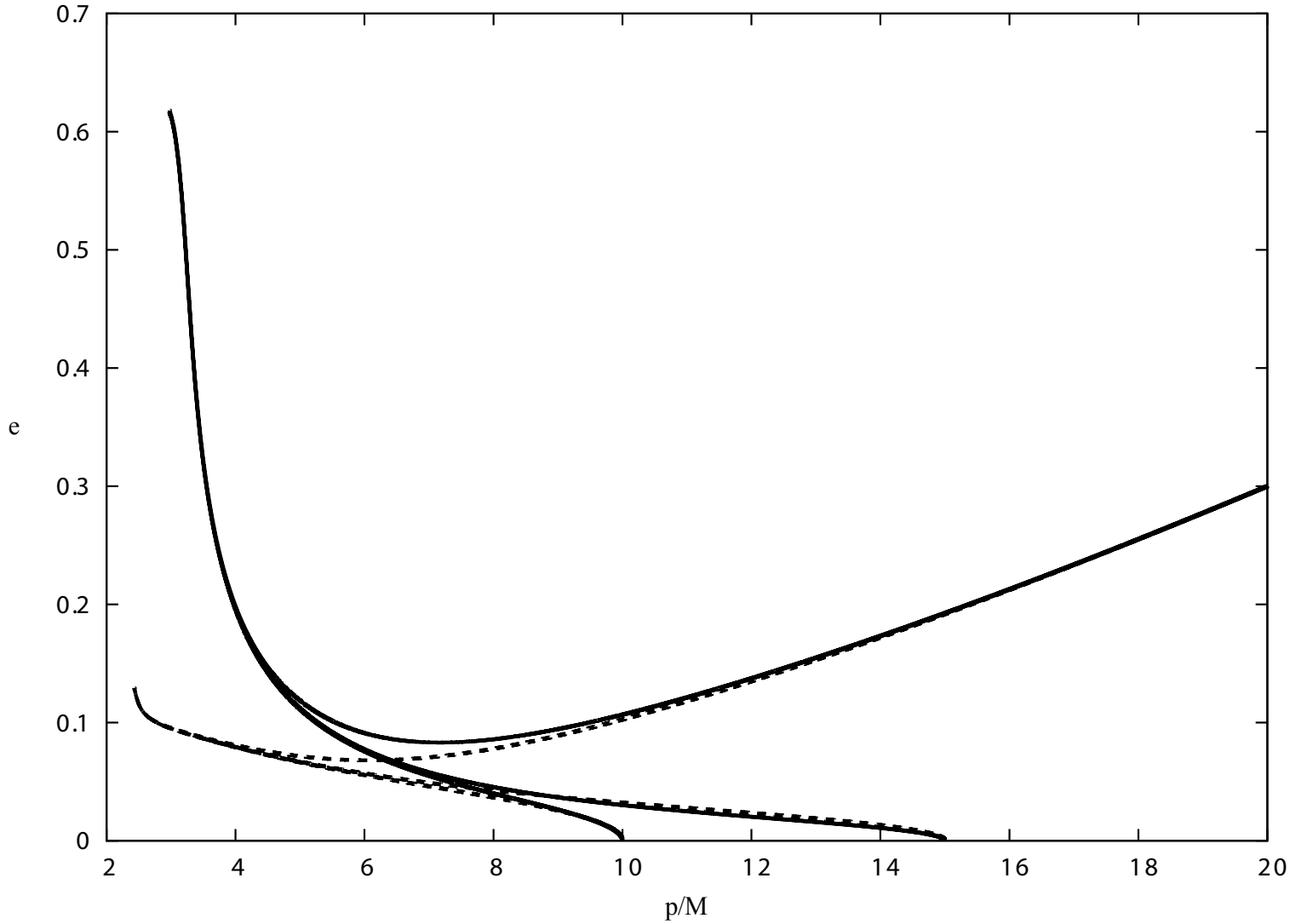

Consistency corrections – near circular orbits

- This problem is present using any approximate prescription of the fluxes. Modify the circular piece of the fluxes to enforce consistency.

Consistency corrections – near circular orbits

- This problem is present using any approximate prescription of the fluxes. Modify the circular piece of the fluxes to enforce consistency.

- Should correct either $\dot{E}$ or $\dot{L}_z$ since $i \equiv 0$ in the equatorial plane. We choose to correct $\dot{L}_z$.

Consistency corrections – near circular orbits

- This problem is present using any approximate prescription of the fluxes. Modify the circular piece of the fluxes to enforce consistency.
- Should correct either $\dot{E}$ or $\dot{L}_z$ since $i \equiv 0$ in the equatorial plane. We choose to correct $\dot{L}_z$.
- Determine circular piece of $\dot{L}_z$ from the $\dot{E}$ and i fluxes. Cannot determine eccentricity corrections, so leave these unchanged. However, do include necessary T_{orb} factor of $(1-e^2)^{-3/2}$.

Near circular orbits – corrected fluxes

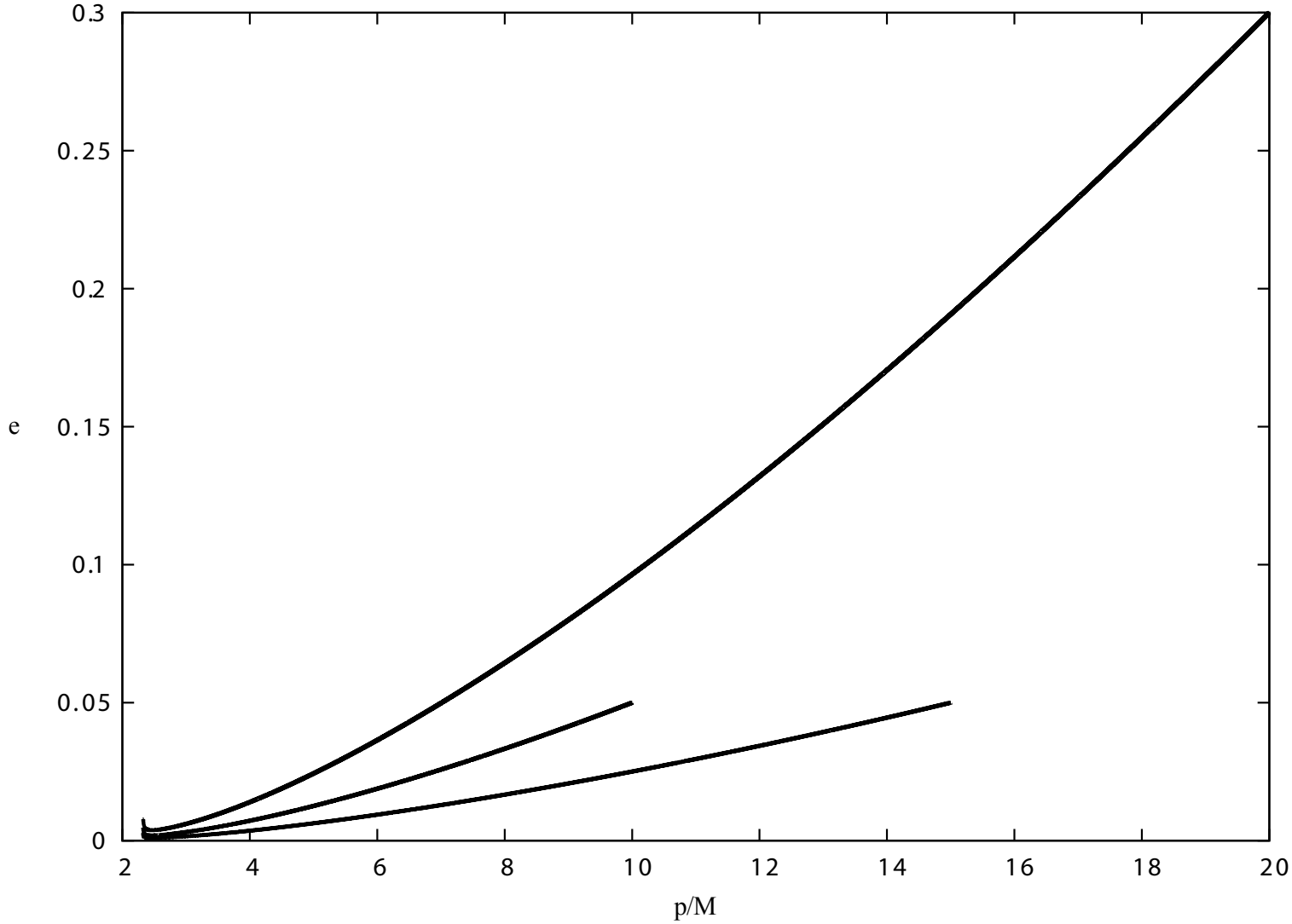

Consistency corrections – near polar orbits

- Find that $\mathrm{d}e/\mathrm{d}t$ expression also diverges as $\iota \to \pi/2$ unless

$$\frac{\mathrm{d}L_z}{\mathrm{d}t}\left(p, e, \iota = \frac{\pi}{2}\right) = -\sqrt{Q\left(p, e, \iota = \frac{\pi}{2}\right)}\frac{\mathrm{d}\iota}{\mathrm{d}t}\left(p, e, \iota = \frac{\pi}{2}\right) \tag{6}$$

Consistency corrections – near polar orbits

- Find that $\mathrm{d}e/\mathrm{d}t$ expression also diverges as $\iota \to \pi/2$ unless

$$\frac{\mathrm{d}L_z}{\mathrm{d}t}\left(p, e, \iota = \frac{\pi}{2}\right) = -\sqrt{Q\left(p, e, \iota = \frac{\pi}{2}\right)}\frac{\mathrm{d}\iota}{\mathrm{d}t}\left(p, e, \iota = \frac{\pi}{2}\right) \tag{6}$$

- The origin of this constraint may be seen by examining $\mathrm{d}Q/\mathrm{d}t$

$$\frac{\mathrm{d}Q}{\mathrm{d}t} = 2\sqrt{Q}\frac{\sin\iota}{\cos\iota}\left(\frac{\mathrm{d}L_z}{\mathrm{d}t} + \sqrt{Q}\frac{1}{\sin^2\iota}\frac{\mathrm{d}\iota}{\mathrm{d}t}\right) \tag{7}$$

Consistency corrections – near polar orbits

- Find that $\mathrm{d}e/\mathrm{d}t$ expression also diverges as $\iota \to \pi/2$ unless

$$\frac{\mathrm{d}L_z}{\mathrm{d}t}\left(p, e, \iota = \frac{\pi}{2}\right) = -\sqrt{Q\left(p, e, \iota = \frac{\pi}{2}\right)}\frac{\mathrm{d}\iota}{\mathrm{d}t}\left(p, e, \iota = \frac{\pi}{2}\right) \tag{6}$$

- The origin of this constraint may be seen by examining $\mathrm{d}Q/\mathrm{d}t$

$$\frac{\mathrm{d}Q}{\mathrm{d}t} = 2\sqrt{Q}\frac{\sin\iota}{\cos\iota}\left(\frac{\mathrm{d}L_z}{\mathrm{d}t} + \sqrt{Q}\frac{1}{\sin^2\iota}\frac{\mathrm{d}\iota}{\mathrm{d}t}\right) \tag{7}$$

- Constraint imposes finiteness on $\mathrm{d}Q/\mathrm{d}t$ – ι is a bad coordinate at the pole, and $i = 0$ is unphysical.

Consistency corrections – near polar orbits

- Find that $\mathrm{d}e/\mathrm{d}t$ expression also diverges as $\iota \to \pi/2$ unless

$$\frac{\mathrm{d}L_z}{\mathrm{d}t}\left(p, e, \iota = \frac{\pi}{2}\right) = -\sqrt{Q\left(p, e, \iota = \frac{\pi}{2}\right)}\frac{\mathrm{d}\iota}{\mathrm{d}t}\left(p, e, \iota = \frac{\pi}{2}\right) \tag{6}$$

- The origin of this constraint may be seen by examining $\mathrm{d}Q/\mathrm{d}t$

$$\frac{\mathrm{d}Q}{\mathrm{d}t} = 2\sqrt{Q}\frac{\sin\iota}{\cos\iota}\left(\frac{\mathrm{d}L_z}{\mathrm{d}t} + \sqrt{Q}\frac{1}{\sin^2\iota}\frac{\mathrm{d}\iota}{\mathrm{d}t}\right) \tag{7}$$

- Constraint imposes finiteness on $\mathrm{d}Q/\mathrm{d}t$ – ι is a bad coordinate at the pole, and $i = 0$ is unphysical.

- Must use a non-zero i and add an additional correction to $\dot{L}_z$ of the form $f(\iota)\,\Delta\dot{L}_z^{pol}$. Use simplest function $f(\iota) = \sin^2(\iota)$. The p dependence of the correction has some additional complications.

Near polar orbits – no correction

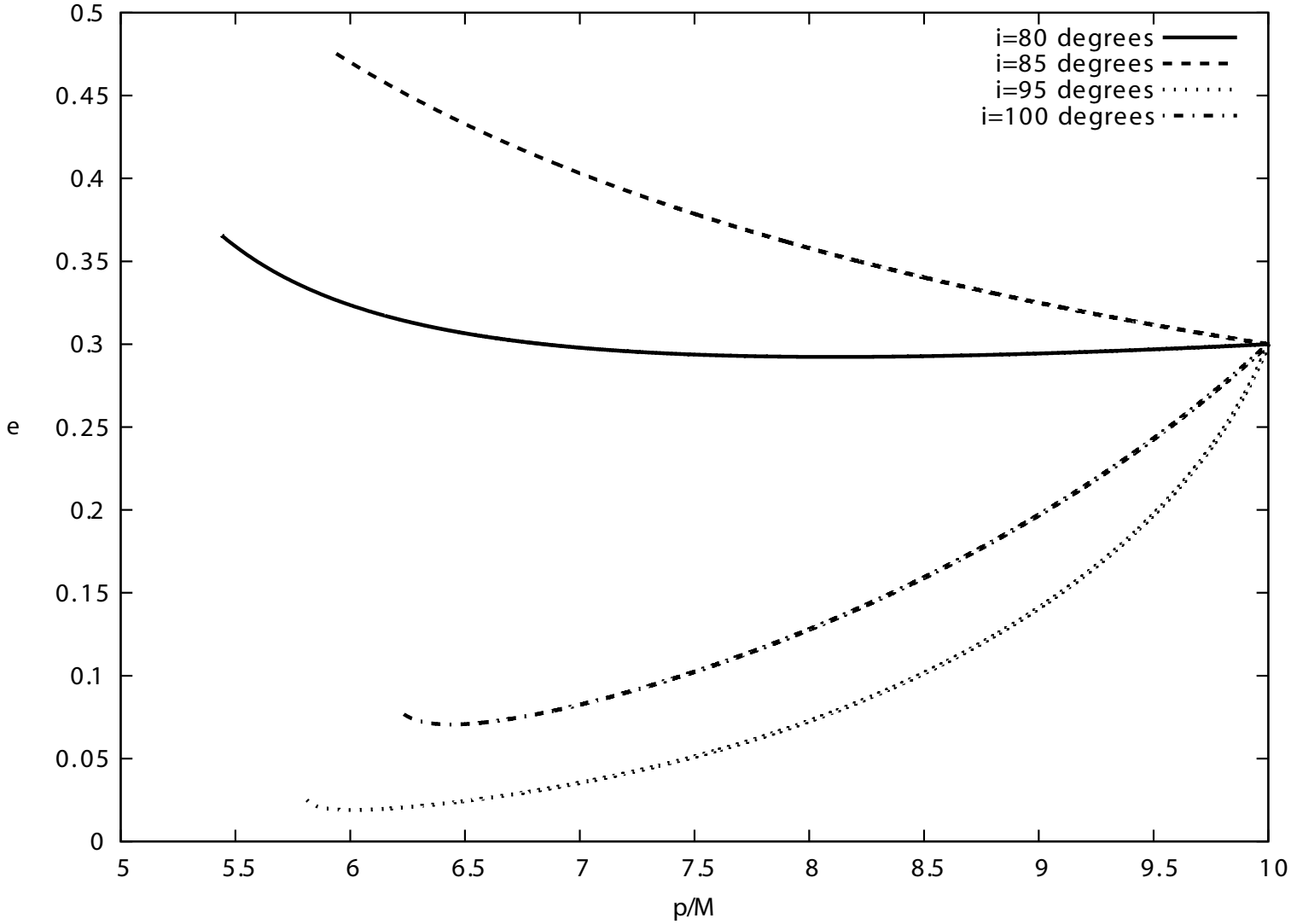

Near polar orbits – corrected fluxes

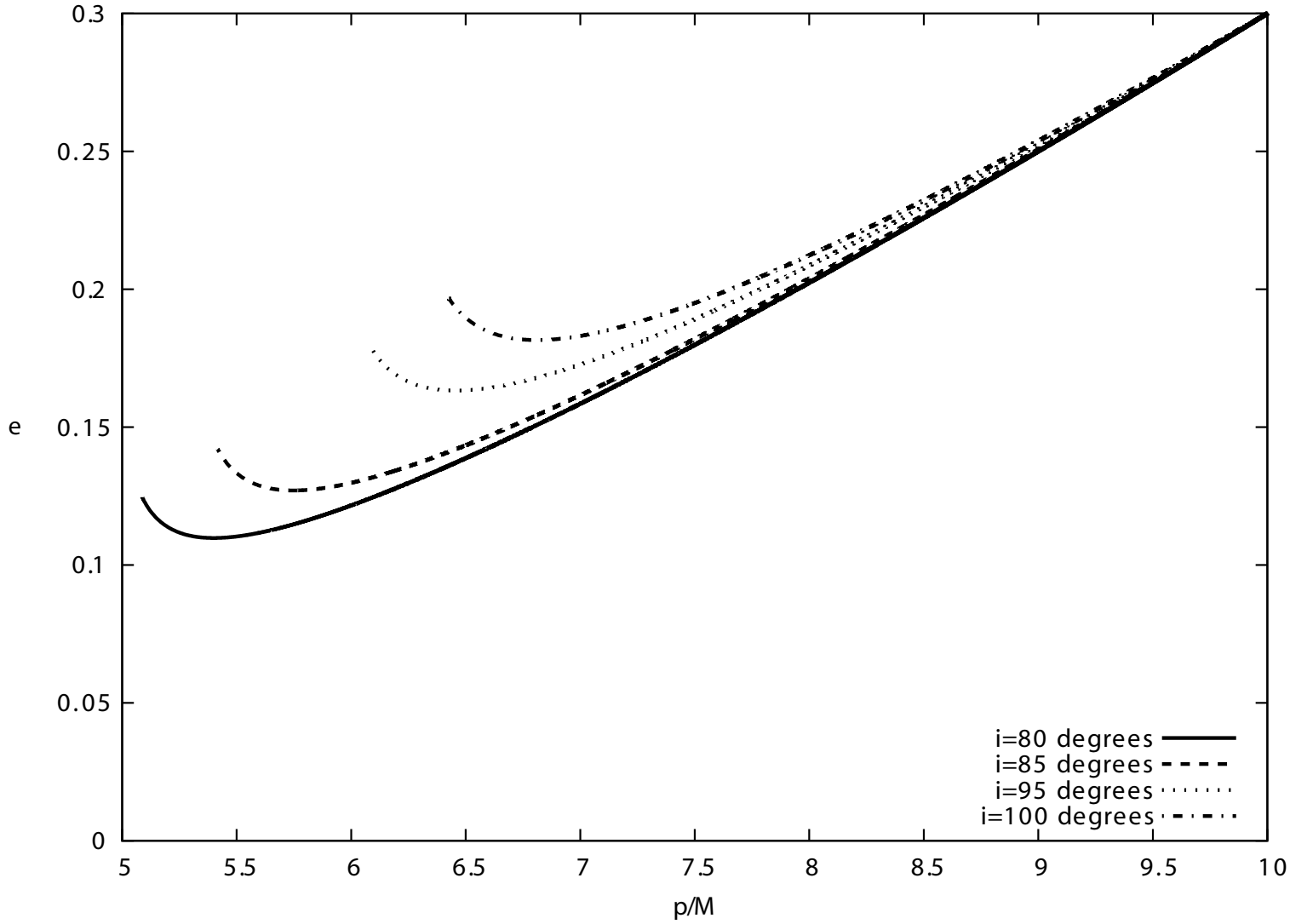

2PN energy and angular momentum fluxes

- Previous corrections are always necessary, but become vanishingly small as the accuracy of the flux expressions improves. Flux expressions at 2.5PN are available for equatorial orbits (Tagoshi 1995) and for low inclination circular orbits (Shibata et al. 1995). Truncate at 2PN for improved accuracy, and extend to arbitrary inclinations in logical way (e.g., $1-\iota^2/2 \to \cos\iota$, $\iota^2 \to \sin^2\iota$).

$$
\begin{aligned}
\dot{E} &= -\frac{32}{5}\frac{\mu^2}{M^2}\left(\frac{M}{p}\right)^5 (1-e^2)^{3/2}\left[g_1(e) - \left(\frac{a}{M}\right)\left(\frac{M}{p}\right)^{3/2} g_2(e)\cos\iota - \left(\frac{M}{p}\right) g_3(e)\right. \\
&\quad \left. +\pi\left(\frac{M}{p}\right)^{3/2} g_4(e) - \left(\frac{M}{p}\right)^2 g_5(e) + \left(\frac{a}{M}\right)^2\left(\frac{M}{p}\right)^2 g_6(e) - \frac{527}{96}\left(\frac{a}{M}\right)^2\left(\frac{M}{p}\right)^2 \sin^2\iota\right] \\
\dot{L}_z &= -\frac{32}{5}\frac{\mu^2}{M}\left(\frac{M}{p}\right)^{7/2} (1-e^2)^{3/2}\left[g_7(e)\cos\iota + \left(\frac{a}{M}\right)\left(\frac{M}{p}\right)^{3/2}\{g_8(e) - \cos^2\iota g_9(e)\}\right. \\
&\quad - \left(\frac{M}{p}\right) g_{10}(e)\cos\iota + \pi\left(\frac{M}{p}\right)^{3/2} g_{11}(e)\cos\iota - \left(\frac{M}{p}\right)^2 g_{12}(e)\cos\iota \\
&\quad \left. + \left(\frac{a}{M}\right)^2\left(\frac{M}{p}\right)^2\left(g_{13}(e) - 2\lambda + \left(\frac{229}{16} - g_7(e) - 3\lambda\right)\cos\iota + \lambda\cos^3\iota\right)\right] \qquad (8)
\end{aligned}
$$

Inclination evolution I – PN results

- The GHK kludge, $i = 0$, is unphysical near the pole, but Ryan's leading order expression for i overpredicts the inclination evolution

$$i = \frac{32}{5}\frac{\mu^3}{M^2}\left(\frac{M}{p}\right)^{\frac{11}{2}}\left(\frac{a}{M}\right)\sin\iota\,(1-e^2)^{3/2}\left(\frac{61}{24}+\frac{63}{8}e^2+\frac{183}{32}e^4\right) \tag{9}$$

Inclination evolution I – PN results

- The GHK kludge, $i = 0$, is unphysical near the pole, but Ryan's leading order expression for i overpredicts the inclination evolution

$$i = \frac{32}{5}\frac{\mu^3}{M^2}\left(\frac{M}{p}\right)^{\frac{11}{2}}\left(\frac{a}{M}\right)\sin\iota\,(1-e^2)^{3/2}\left(\frac{61}{24}+\frac{63}{8}e^2+\frac{183}{32}e^4\right) \tag{9}$$

- In fact, Ryan's expression can be derived from the polar consistency correction. By extension, can use the 2PN $\dot{L}_z$ expression to determine pieces of i that do not vanish at $\iota = \pi/2$. The true i will also contain terms proportional to $\cos\iota$. Therefore, use the ansatz

$$i = \frac{32}{5}\frac{\mu^3}{Q}\left(\frac{M}{p}\right)^{\frac{9}{2}}\left(\frac{a}{M}\right)\sin^3\iota\,(1-e^2)^{3/2}\left(\frac{61}{24}+\frac{63}{8}e^2+\frac{95}{64}e^4+\frac{a}{M}\left(\frac{123}{8}+\frac{41}{8}e^2-2\lambda+\kappa\,\cos\iota\right)\right) \tag{10}$$

Inclination evolution I – PN results

- The GHK kludge, $i = 0$, is unphysical near the pole, but Ryan's leading order expression for i overpredicts the inclination evolution

$$i = \frac{32}{5}\frac{\mu^3}{M^2}\left(\frac{M}{p}\right)^{\frac{11}{2}}\left(\frac{a}{M}\right)\sin\iota\,(1-e^2)^{3/2}\left(\frac{61}{24}+\frac{63}{8}e^2+\frac{183}{32}e^4\right) \tag{9}$$

- In fact, Ryan's expression can be derived from the polar consistency correction. By extension, can use the 2PN $\dot{L}_z$ expression to determine pieces of i that do not vanish at $\iota = \pi/2$. The true i will also contain terms proportional to $\cos\iota$. Therefore, use the ansatz

$$i = \frac{32}{5}\frac{\mu^3}{Q}\left(\frac{M}{p}\right)^{\frac{9}{2}}\left(\frac{a}{M}\right)\sin^3\iota\,(1-e^2)^{3/2}\left(\frac{61}{24}+\frac{63}{8}e^2+\frac{95}{64}e^4+\frac{a}{M}\left(\frac{123}{8}+\frac{41}{8}e^2-2\lambda+\kappa\,\cos\iota\right)\right) \tag{10}$$

- Circular Teukolsky results indicate $\lambda = 7.380$, $\kappa = -3.315$ is a good approximation.

Inclination evolution I – PN results

- The GHK kludge, $i = 0$, is unphysical near the pole, but Ryan's leading order expression for i overpredicts the inclination evolution

$$i = \frac{32}{5}\frac{\mu^3}{M^2}\left(\frac{M}{p}\right)^{\frac{11}{2}}\left(\frac{a}{M}\right)\sin\iota\,(1-e^2)^{3/2}\left(\frac{61}{24}+\frac{63}{8}e^2+\frac{183}{32}e^4\right) \tag{9}$$

- In fact, Ryan's expression can be derived from the polar consistency correction. By extension, can use the 2PN $\dot{L}_z$ expression to determine pieces of i that do not vanish at $\iota = \pi/2$. The true i will also contain terms proportional to $\cos\iota$. Therefore, use the ansatz

$$i = \frac{32}{5}\frac{\mu^3}{Q}\left(\frac{M}{p}\right)^{\frac{9}{2}}\left(\frac{a}{M}\right)\sin^3\iota\,(1-e^2)^{3/2}\left(\frac{61}{24}+\frac{63}{8}e^2+\frac{95}{64}e^4+\frac{a}{M}\left(\frac{123}{8}+\frac{41}{8}e^2-2\lambda+\kappa\,\cos\iota\right)\right) \tag{10}$$

- Circular Teukolsky results indicate $\lambda = 7.380$, $\kappa = -3.315$ is a good approximation.

- A PN expression for $\mathrm{d}Q/\mathrm{d}t$ may soon be available for low inclination and low eccentricity orbits – use this to check or improve this prescription.

Inclination evolution II – Teukolsky fit

- The magnitude of i has been computed for circular, inclined orbits by solution of the Teukolsky equation (Hughes 2000). Can use these to construct fits for i.

Inclination evolution II – Teukolsky fit

- The magnitude of i has been computed for circular, inclined orbits by solution of the Teukolsky equation (Hughes 2000). Can use these to construct fits for i.
- At $p = 10$, find a good fit of the form

$$\frac{\mathrm{d}\iota}{\mathrm{d}t} = \frac{32}{5}\frac{\mu^3}{M^4} c_0 \left(\frac{a}{M}\right) \sin\iota \left(c_1 + \frac{a}{M} c_2 \cos\iota + \left(\frac{a}{M}\right)^2 (c_3 + c_4 \cos^2\iota) + \left(\frac{a}{M}\right)^3 c_5 \cos\iota\right) \quad (11)$$

- Coefficients in this expansion are dependent on orbital radius, p. Can guess the form of this dependence, but will determine it from additional Teukolsky data.

Inclination evolution II – Teukolsky fit

- The magnitude of i has been computed for circular, inclined orbits by solution of the Teukolsky equation (Hughes 2000). Can use these to construct fits for i.

- At $p = 10$, find a good fit of the form

$$\frac{\mathrm{d}\iota}{\mathrm{d}t} = \frac{32}{5}\frac{\mu^3}{M^4} c_0 \left(\frac{a}{M}\right) \sin\iota \left(c_1 + \frac{a}{M} c_2 \cos\iota + \left(\frac{a}{M}\right)^2 (c_3 + c_4 \cos^2\iota) + \left(\frac{a}{M}\right)^3 c_5 \cos\iota \right) \quad (11)$$

- Coefficients in this expansion are dependent on orbital radius, p. Can guess the form of this dependence, but will determine it from additional Teukolsky data.

- Does not give the eccentricity dependent pieces – must use PN expressions. Once generic data is available, can revisit this fit.

Inclination evolution II – Teukolsky data

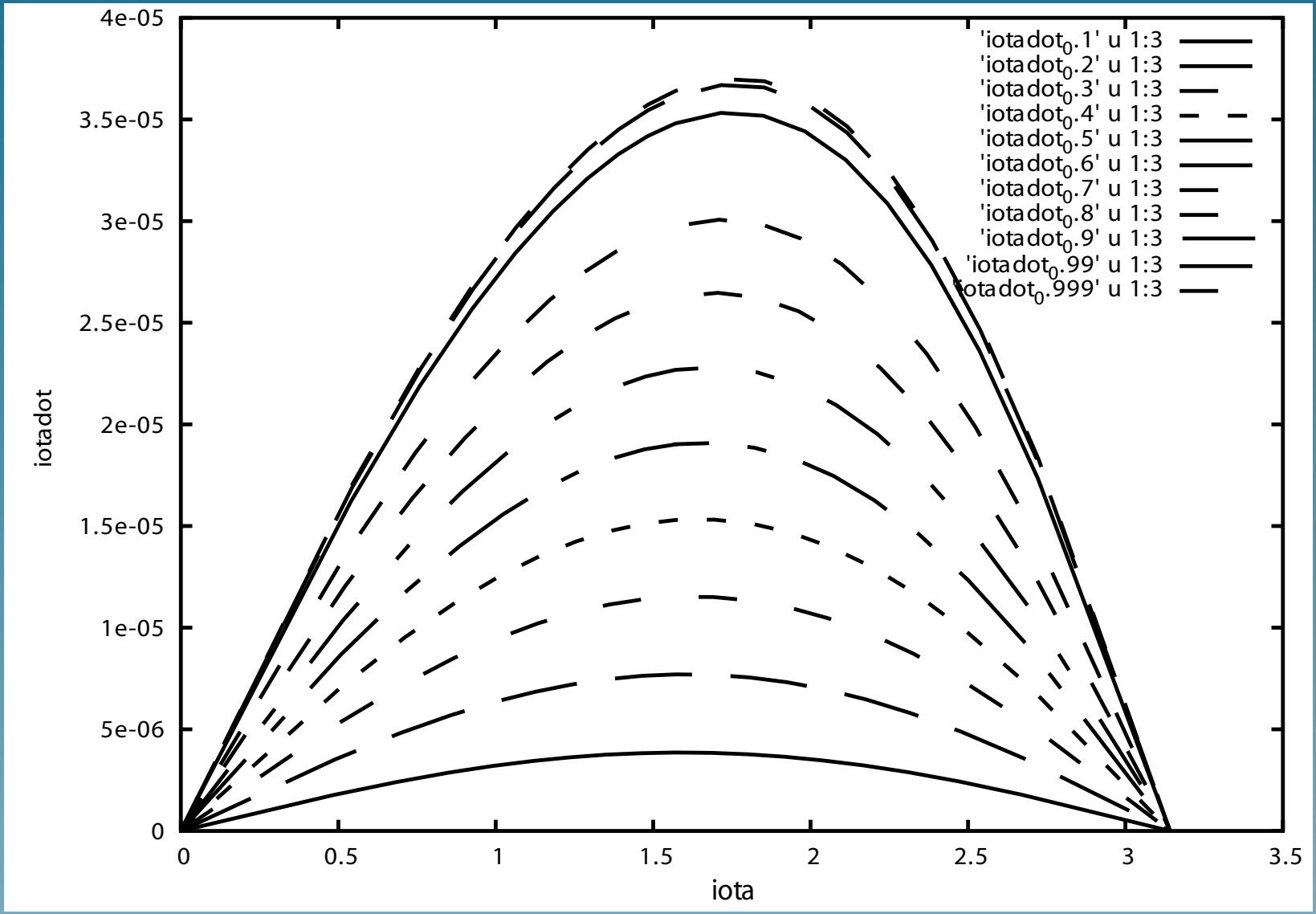

Inclination evolution II – fit to Teukolsky data

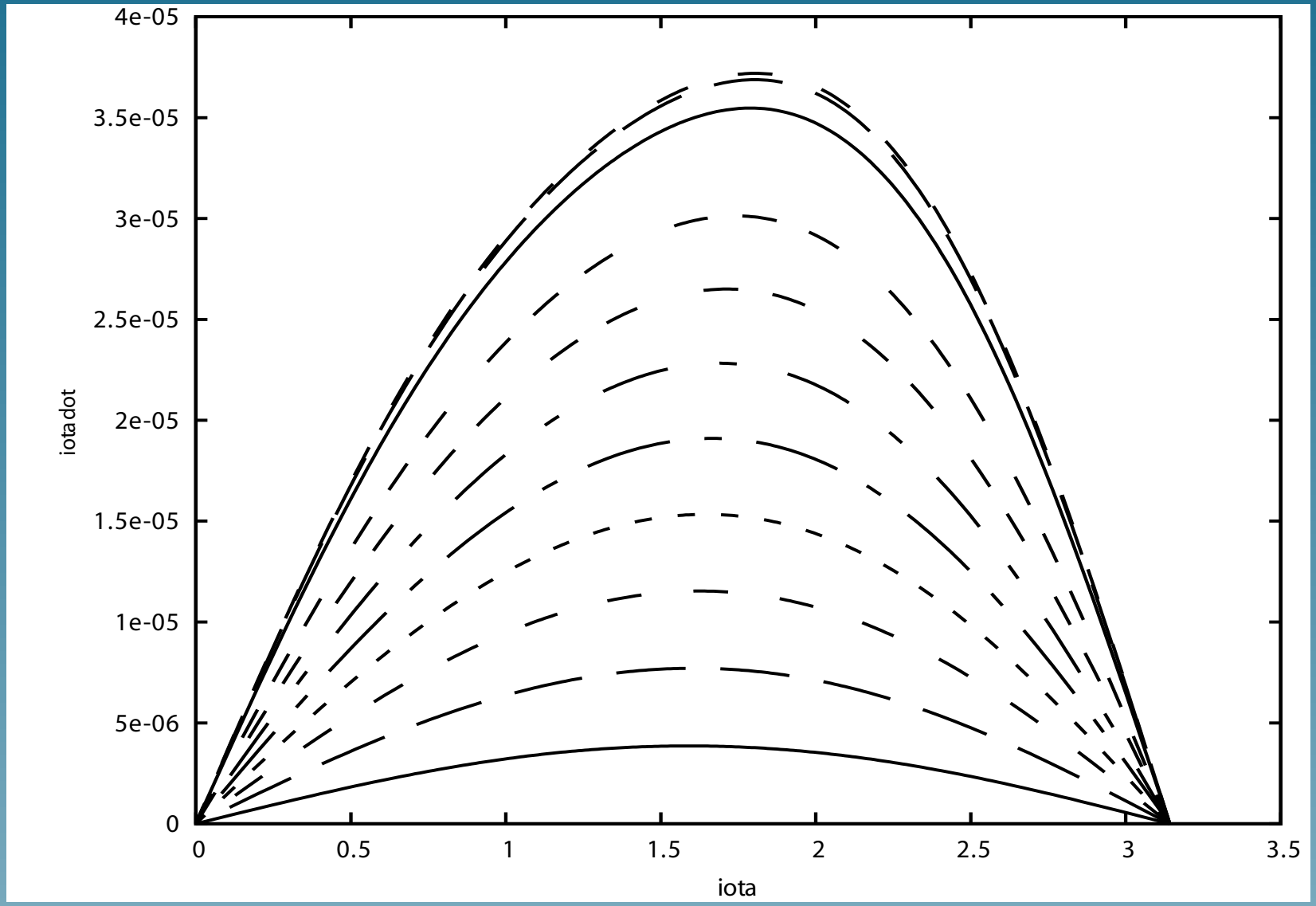

Waveform generation

- Define pseudo-Cartesian coordinates from Boyer-Lindquist (r, θ, ϕ) by

$$x = r\ \sin\theta\ \cos\phi, \qquad y = r\ \sin\theta\ \sin\phi, \qquad z = r\ \cos\theta \tag{12}$$

Waveform generation

- Define pseudo-Cartesian coordinates from Boyer-Lindquist (r, θ, ϕ) by

$$x = r\,\sin\theta\,\cos\phi, \qquad y = r\,\sin\theta\,\sin\phi, \qquad z = r\,\cos\theta \tag{12}$$

- Construct flat-space quadrupole moment tensor based on these coordinates

$$\mathcal{I}^{ij} = x^i(t)\,x^j(t) - \frac{1}{3}\,\delta^{ij}\,r^2(t), \qquad h^{ij} = \frac{2}{r}\,\frac{\mathrm{d}^2}{\mathrm{d}t^2}\,\mathcal{I}^{ij}. \tag{13}$$

Waveform generation

- Define pseudo-Cartesian coordinates from Boyer-Lindquist (r, θ, ϕ) by

$$x = r\,\sin\theta\,\cos\phi, \qquad y = r\,\sin\theta\,\sin\phi, \qquad z = r\,\cos\theta \tag{12}$$

- Construct flat-space quadrupole moment tensor based on these coordinates

$$\mathcal{I}^{ij} = x^i(t)\,x^j(t) - \frac{1}{3}\,\delta^{ij}\,r^2(t), \qquad h^{ij} = \frac{2}{r}\,\frac{\mathrm{d}^2}{\mathrm{d}t^2}\,\mathcal{I}^{ij}. \tag{13}$$

- These waveforms are purely quadrupolar. Can include approximations to other multipoles in a similar way – quadrupole/octupole waveforms, Press waveforms (weak field, fast motion approximation).

Tests – comparison to perturbative results

- Compare kludge fluxes to circular inclined and eccentric equatorial (and soon generic) Teukolsky computations. For example, circular orbits with $\iota = 60^{\rm o}$.

$\frac{p}{M}$	$\frac{a}{M}$	$\lvert\dot{E}^T - \dot{E}^K\rvert/\dot{E}^T$	$\lvert\dot{L_z}^T - \dot{L_z}^K\rvert/\dot{L_z}^T$	$\lvert i^T - i^K\rvert/i^T$
7	0.05	0.0018	0.00022	0.18
7	0.95	0.064	0.062	0.048
100	0.05	0.00025	0.00025	0.017
100	0.95	0.00022	0.00018	0.013

Tests – comparison to perturbative results

- Compare kludge fluxes to circular inclined and eccentric equatorial (and soon generic) Teukolsky computations. For example, circular orbits with $\iota = 60^{\rm o}$.

$\frac{p}{M}$	$\frac{a}{M}$	$\lvert\dot{E}^T - \dot{E}^K\rvert/\dot{E}^T$	$\lvert\dot{L_z}^T - \dot{L_z}^K\rvert/\dot{L_z}^T$	$\lvert i^T - i^K\rvert/i^T$
7	0.05	0.0018	0.00022	0.18
7	0.95	0.064	0.062	0.048
100	0.05	0.00025	0.00025	0.017
100	0.95	0.00022	0.00018	0.013

- Compute overlaps of (geodesic) kludge waveforms with Teukolsky based waveforms.

p	e	a	overlap	p	ι	a	overlap
1.7	0.1	0.99	0.741	5	30	0.5	0.990
1.7	0.3	0.99	0.500	5	30	0.99	0.973
2.5	0.1	0.99	0.827	5	60	0.99	0.888
2.5	0.5	0.99	0.651	10	30	0.5	0.990
5.1	0.5	0.5	0.967	10	30	0.99	0.982
10	0.3	-0.99	0.966	10	60	0.99	0.937

Tests – comparison to perturbative results

- Compare kludge fluxes to circular inclined and eccentric equatorial (and soon generic) Teukolsky computations. For example, circular orbits with $\iota = 60^{\rm o}$.

$\frac{p}{M}$	$\frac{a}{M}$	$\lvert\dot{E}^T - \dot{E}^K\rvert/\dot{E}^T$	$\lvert\dot{L_z}^T - \dot{L_z}^K\rvert/\dot{L_z}^T$	$\lvert i^T - i^K\rvert/i^T$
7	0.05	0.0018	0.00022	0.18
7	0.95	0.064	0.062	0.048
100	0.05	0.00025	0.00025	0.017
100	0.95	0.00022	0.00018	0.013

- Compute overlaps of (geodesic) kludge waveforms with Teukolsky based waveforms.

p	e	a	overlap	p	ι	a	overlap
1.7	0.1	0.99	0.741	5	30	0.5	0.990
1.7	0.3	0.99	0.500	5	30	0.99	0.973
2.5	0.1	0.99	0.827	5	60	0.99	0.888
2.5	0.5	0.99	0.651	10	30	0.5	0.990
5.1	0.5	0.5	0.967	10	30	0.99	0.982
10	0.3	-0.99	0.966	10	60	0.99	0.937

- Compare spectrum of radiation to Teukolsky results – the frequencies represented in the kludge spectrum are correct but many modes are absent.

Tests – kludge waveform spectrum

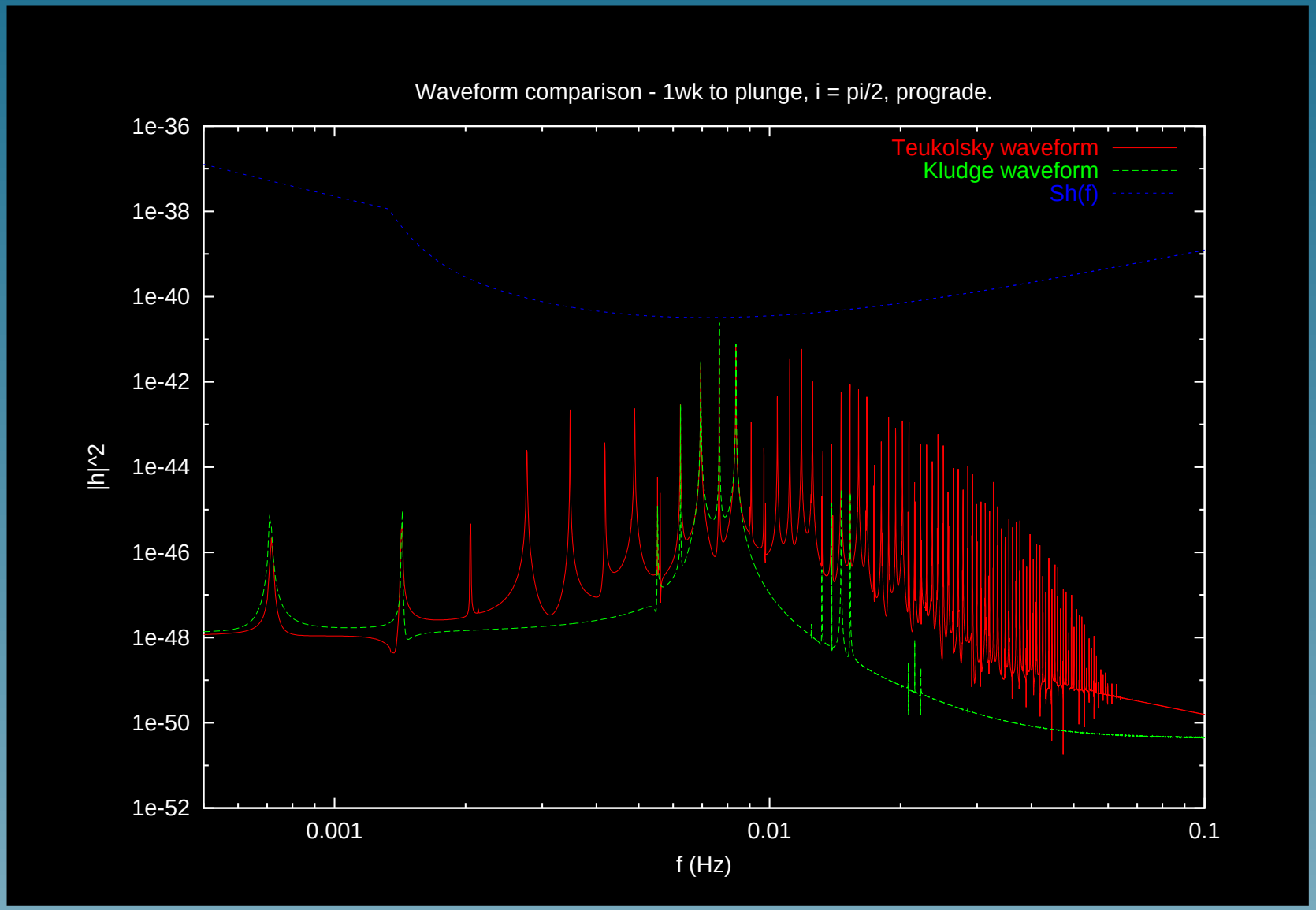

Tests – stability of near-circular orbits

- Near $e = 0$, $\mathrm{d}e/\mathrm{d}t \approx f(p, \iota)\, e$. Locus of points where $f(p, \iota) = 0$ is important for determining properties of inspirals. Kennefick (1998) computed the location of this point in the equatorial plane as a function of spin. Repeating this calculation, we agree to $\sim 4\%$.

Tests – stability of near-circular orbits

- Near $e = 0$, $\mathrm{d}e/\mathrm{d}t \approx f(p, \iota)\, e$. Locus of points where $f(p, \iota) = 0$ is important for determining properties of inspirals. Kennefick (1998) computed the location of this point in the equatorial plane as a function of spin. Repeating this calculation, we agree to $\sim 4\%$.

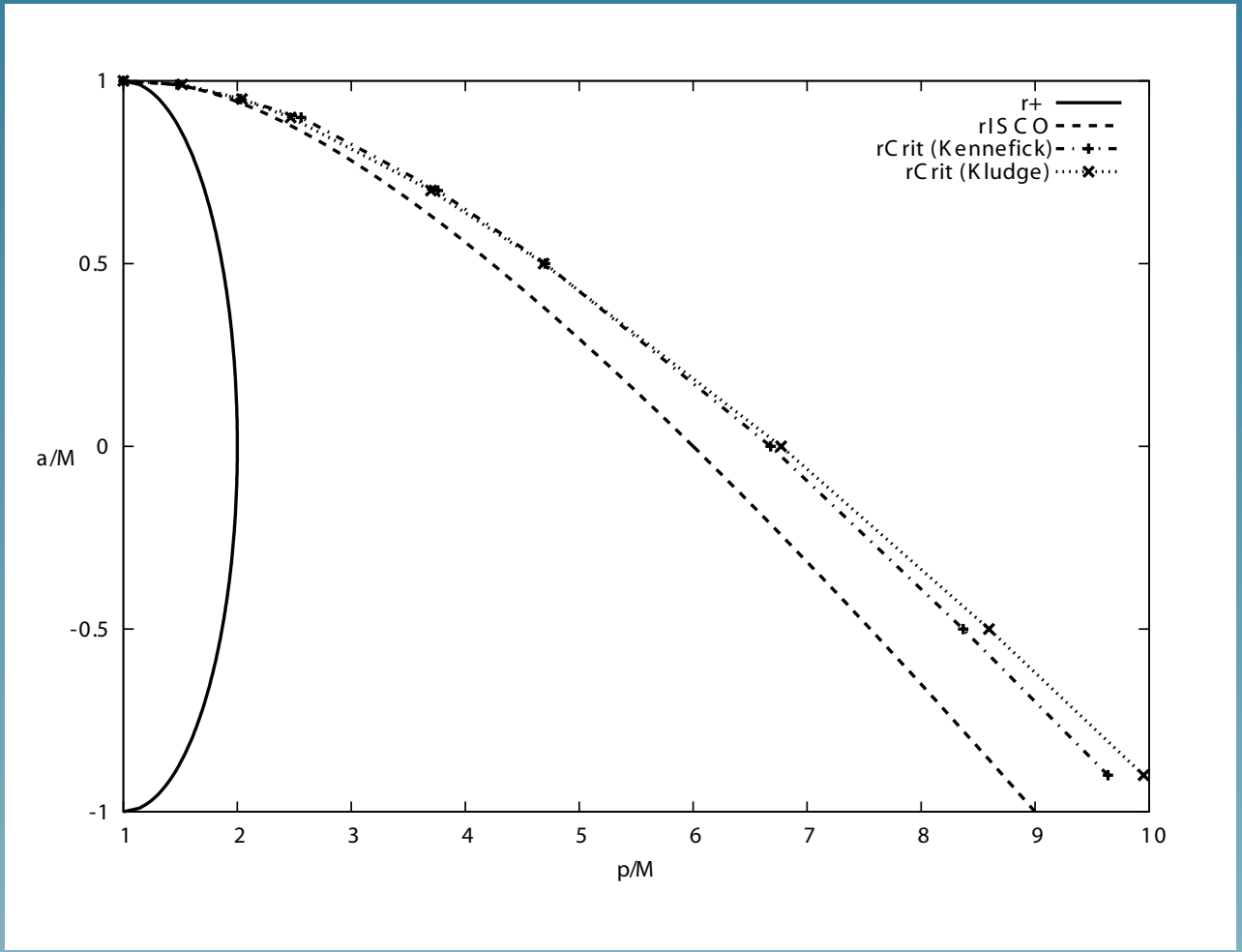

Applications – computing inspiral trajectories

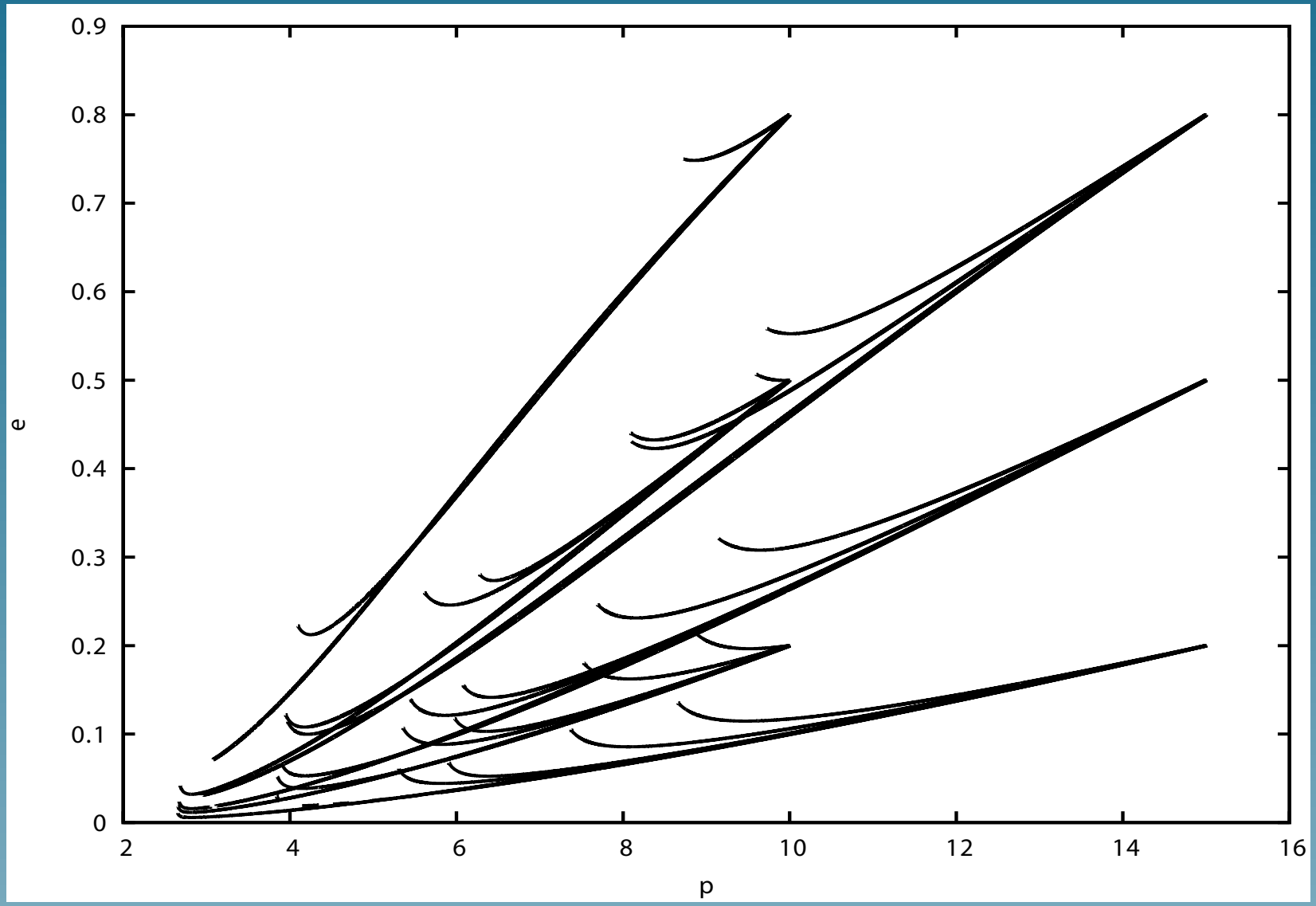

Applications – computing inspiral trajectories

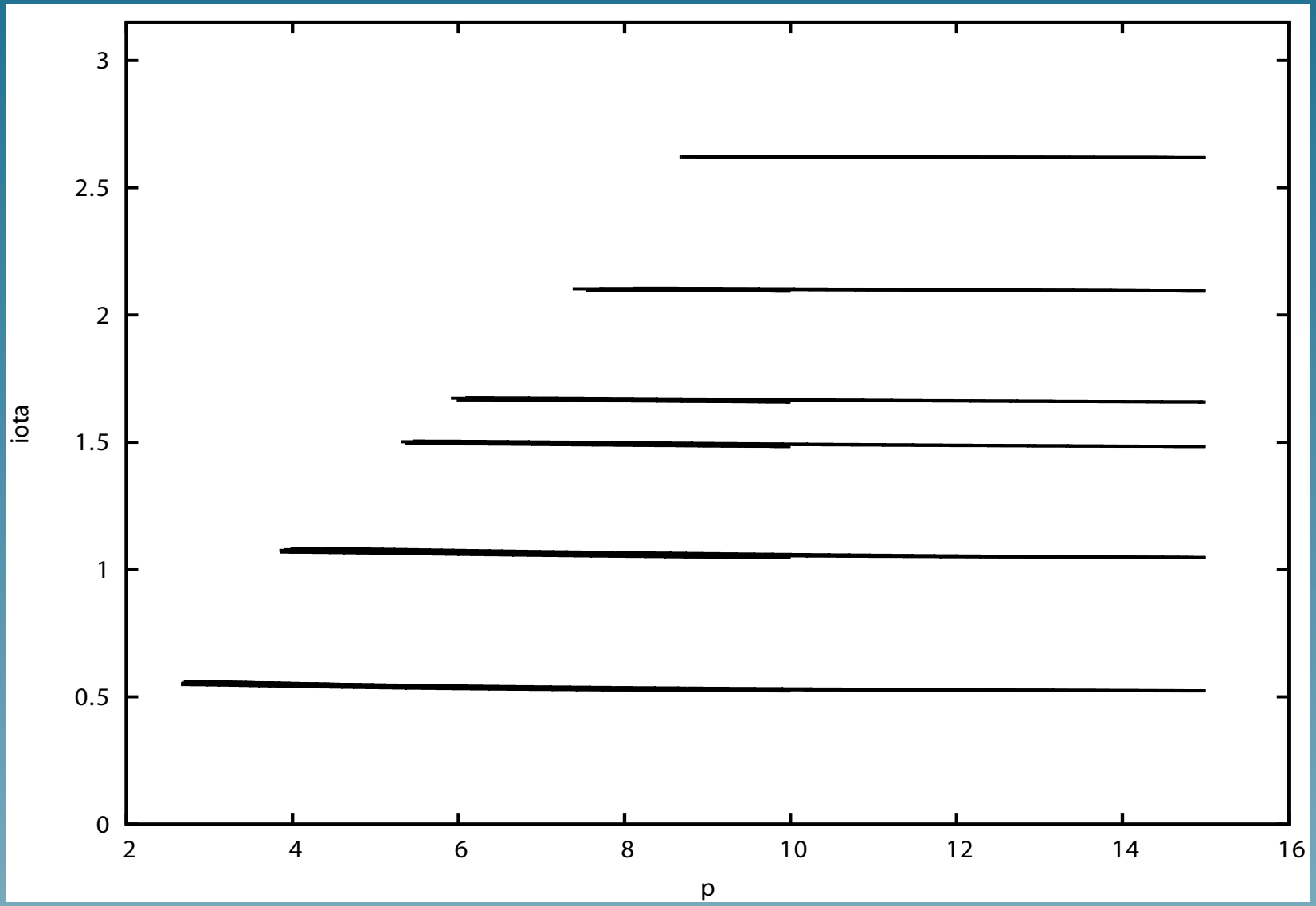

Applications – SNR computations

- Computes matched filtering SNR's for LISA EMRI detections by using kludged waveforms in conjunction with "Synthetic LISA". Important computation for estimating detection rates.

Applications – SNR computations

- Computes matched filtering SNR's for LISA EMRI detections by using kludged waveforms in conjunction with "Synthetic LISA". Important computation for estimating detection rates.

M	m	S/N(AET)						S/N(X)					
		(1wk)	(1mo)	(3mo)	(1yr)	(3yr)	(5yr)	(1wk)	(1mo)	(3mo)	(1yr)	(3yr)	(5yr)
$3 \cdot 10^5$	0.6	1.1	3.0	5.1	10.2	16.8	20.4	0.6	1.6	2.2	5.8	10.2	12.6
$3 \cdot 10^5$	10	27.8	60.3	80.4	119.0	149.0	162.0	16.6	38.0	48.8	74.7	95.4	104.0
$3 \cdot 10^5$	100	277.0	440.0	508.0	591.0	626.0	633.0	188.0	300.0	338.0	391.0	414.0	419.0
10^6	0.6	3.7	7.3	10.0	18.5	29.0	34.9	2.5	4.9	6.3	12.0	19.0	23.0
10^6	10	58.2	109.0	140.0	205.0	252.0	271.0	40.5	75.5	92.9	136.0	168.0	181.0
10^6	100	477.0	752.0	860.0	989.0	1060.0	1090.0	338.0	532.0	595.0	678.0	727.0	743.0
$3 \cdot 10^6$	0.6	3.1	6.0	8.0	14.1	21.2	24.9	2.2	4.2	5.4	9.5	14.3	16.7
$3 \cdot 10^6$	10	45.7	81.8	102.0	138.0	158.0	164.0	32.7	57.8	69.8	93.9	107.0	111.0
$3 \cdot 10^6$	100	344.0	508.0	559.0	590.0	601.0	604.0	244.0	360.0	391.0	411.0	418.0	420.0

Applications – SNR computations

- Computes matched filtering SNR's for LISA EMRI detections by using kludged waveforms in conjunction with "Synthetic LISA". Important computation for estimating detection rates.

M	m	S/N(AET)						S/N(X)					
		(1wk)	(1mo)	(3mo)	(1yr)	(3yr)	(5yr)	(1wk)	(1mo)	(3mo)	(1yr)	(3yr)	(5yr)
$3 \cdot 10^5$	0.6	1.1	3.0	5.1	10.2	16.8	20.4	0.6	1.6	2.2	5.8	10.2	12.6
$3 \cdot 10^5$	10	27.8	60.3	80.4	119.0	149.0	162.0	16.6	38.0	48.8	74.7	95.4	104.0
$3 \cdot 10^5$	100	277.0	440.0	508.0	591.0	626.0	633.0	188.0	300.0	338.0	391.0	414.0	419.0
10^6	0.6	3.7	7.3	10.0	18.5	29.0	34.9	2.5	4.9	6.3	12.0	19.0	23.0
10^6	10	58.2	109.0	140.0	205.0	252.0	271.0	40.5	75.5	92.9	136.0	168.0	181.0
10^6	100	477.0	752.0	860.0	989.0	1060.0	1090.0	338.0	532.0	595.0	678.0	727.0	743.0
$3 \cdot 10^6$	0.6	3.1	6.0	8.0	14.1	21.2	24.9	2.2	4.2	5.4	9.5	14.3	16.7
$3 \cdot 10^6$	10	45.7	81.8	102.0	138.0	158.0	164.0	32.7	57.8	69.8	93.9	107.0	111.0
$3 \cdot 10^6$	100	344.0	508.0	559.0	590.0	601.0	604.0	244.0	360.0	391.0	411.0	418.0	420.0

- Caveat – the numerical kludge inspirals are inconsistent in the sense that the energy and angular momentum carried by the kludge gravitational waves differs from the change in energy and angular momentum of the orbit. This leads to an error in the estimated SNRs.

Applications – scoping out LISA data analysis

- Detection of EMRIs with LISA is hard. Fully coherent matched filtering is impossible due to huge number of templates required. Will use alternative techniques instead (talks tomorrow).

Applications – scoping out LISA data analysis

- Detection of EMRIs with LISA is hard. Fully coherent matched filtering is impossible due to huge number of templates required. Will use alternative techniques instead (talks tomorrow).

- To assess computational requirements of alternative algorithms, need to compute metrics on waveform space – requires many waveform evaluations. Kludge techniques are the only practical way to do this.

Applications – scoping out LISA data analysis

- Detection of EMRIs with LISA is hard. Fully coherent matched filtering is impossible due to huge number of templates required. Will use alternative techniques instead (talks tomorrow).

- To assess computational requirements of alternative algorithms, need to compute metrics on waveform space – requires many waveform evaluations. Kludge techniques are the only practical way to do this.

- We carried out this analysis using the analytic and numerical kludge approaches in parallel. Final counts agreed to a few tens of percent, which provides us with confidence in our results.

Applications – scoping out LISA data analysis

- Detection of EMRIs with LISA is hard. Fully coherent matched filtering is impossible due to huge number of templates required. Will use alternative techniques instead (talks tomorrow).

- To assess computational requirements of alternative algorithms, need to compute metrics on waveform space – requires many waveform evaluations. Kludge techniques are the only practical way to do this.

- We carried out this analysis using the analytic and numerical kludge approaches in parallel. Final counts agreed to a few tens of percent, which provides us with confidence in our results.

- Conclusions – a 50 Teraflop computer running in real time can perform a semi-coherent search using $2-3$ week waveform segments. Threshold SNR for detection is then ~ 35 (over LISA mission), giving 100's of EMRI detections during the mission.

Potential future developments

- Improve phase space trajectories further – use higher order PN expressions or compute fits to perturbative data for $\dot{E}$, $\dot{L}_z$ and i as these become available. (To quote Nakano - Hikida at next Capra meeting!). Improve kludge for waveforms if possible.

- Include conservative contributions – can be implemented easily in the numerical kludge by modifying the geodesic equations.

- Compare against adiabatic and self-force waveforms to assess how well kludge waveforms can match true inspirals. It may be possible to use approximate waveforms as detection templates for LISA in the first stages of the search (phase accuracy needed over a few weeks only). This will greatly simplify the generation of search templates.

Summary

- We have techniques for constructing approximate EMRI waveforms to use in scoping out data analysis for LISA. Resulting waveforms compare favourably to more accurate perturbative calculations.

- Phase space trajectory is computed using PN expressions, but must include corrections to ensure consistent behaviour for nearly circular and nearly polar inspirals.

- Kludge waveforms have proven useful for scoping out semi-coherent and other techniques for LISA data analysis and for estimating LISA detection rates.

- The approximation can be improved further and some variant might be useful in searches for EMRIs in the actual LISA data.